Fractional Hammerstein Modeling of the Heating Process With Exponential Static Nonlinearity Identified Via The Honey Badger Approach

DHOUHA CHOUAIBI, WASSILA CHAGRA
Analysis, Conception and Control of Systems Laboratory,
University El Manar, National Engineering School of Tunis,
BP N◦ 37 Belvedere 1002, Tunis,
TUNISIA

Abstract: - Many thermal processes encountered in real applications display nonlinear behaviors that conventional linear models fail to represent with sufficient accuracy. This limitation highlights the need for more flexible hybrid modeling approaches, such as fractional Hammerstein structures. In this work, a thermal system is modeled using a fractional Hammerstein architecture in which the linear dynamic block is formulated as a fractional-order transfer function, while the static nonlinear block is described by an exponential function. To overcome the associated identification challenges, the recently developed Honey Badger metaheuristic optimization algorithm is employed, offering enhanced convergence properties and improved robustness compared with classical optimization approaches. Experimental data are collected from an electric oven using an STM32F407VG microcontroller, ensuring reliable real-time measurements required for accurate model identification.

Key-Words: - Fractional Hammerstein structure, Optimization method, Fractional order system, Nonlinear system, Hybrid modeling, Identification, Thermal system.

Received: March 7, 2026. Revised: April 21, 2026. Accepted: May 16, 2026. Published: September 15, 2026.

1 Introduction

Fractional-order models have emerged as powerful tools for representing the dynamics of both linear and nonlinear systems. Fractional formulations offer additional precision due to the accurate description of memory effects and long-range temporal dependencies commonly observed in real physical processes. Over the past decades, numerous research studies have highlighted the effectiveness of fractional models in a wide range of applications, including thermal [1], biological [2], mechanical [3], and electrochemical systems[4].

Nonlinear fractional models proposed in the literature can be categorized into several fundamental classes, such as Volterra series models[5], neural network based structures [6],[7], and block-structured models [8],[9],[10]. Among these, block-structured architectures are widely used due to their clarity of interpretation and their suitability for identifying complex systems. Within this family, the Hammerstein model is one of the most widely used structures. It consists of a static nonlinear block followed by a dynamic linear block expressed through a fractional-order transfer function.

Fractional-order Hammerstein models (FOHM) [11],[12],[13], in particular, have received increasing attention in recent years because of their modeling flexibility and their ability to approximate real processes with high fidelity. They have been successfully applied to various domains, notably in the modeling of thermal [14],[15] and mechanical systems [16]. Their capacity to incorporate static nonlinearities while maintaining a tractable linear fractional dynamic model makes them especially suitable for systems exhibiting both memory effects and nonlinear responses.

The principal methods employed for identifying the parameters of a FOHM are generally classified into two distinct categories. The first group includes optimization techniques, widely employed due to the nonlinear, non-convex, and multi-parametric nature of fractional Hammerstein structures. This family encompasses algorithms inspired by collective or animal behavior, such as the Particle Swarm Optimization (PSO)[17],[18], Genetic Algorithms (GA) [19],[20], and the Grey Wolf Optimizer (GWO) [21]. These methods enable a global search within a complex parameter space, simultaneously handling the identification of both the nonlinear static block and the fractional linear dynamic block. The second category consists of recursive methods, suitable for sequential or iterative parameter estimation when time-series data are available. This group includes variants of Recursive Least Squares (RLS) [22],[23] and the recursive Levenberg Marquardt algorithm [24], which are particularly effective for online identification or for models that allow progressive estimation of the nonlinear and fractional linear components.

The nonlinear part of a Hammerstein model can be represented using various types of functions. The most commonly employed in the literature is the polynomial nonlinearity [25],[26], [27], mainly due to its simplicity in analysis and ease of implementation on digital computers. However, this approach has a significant limitation: the static characteristic, which represents the relationship between the input and output of the nonlinear block, can exhibit multiple extrema as the polynomial degree increases.

Such a configuration becomes problematic when the model is used within control algorithms based on cost function minimization, such as predictive control. Indeed, the presence of multiple extrema leads to a non-convex optimization problem, meaning that a single output may correspond to multiple possible controls.

Main contributions:

– The first contribution of this paper is the use of an exponential function to model the nonlinear part of the Hammerstein model. This avoids these ambiguities and ensures a monotonic behavior that is better suited for optimization-based control methods.

– The second contribution of this paper is the application of the recent Honey Badger Algorithm (HBA) for the identification of FOHM. This approach is particularly well-suited for FOHM, as the algorithm can simultaneously estimate all model parameters, including those of the fractional linear block and the static nonlinear block. Consequently, it combines robustness, the ability to handle complex nonlinearities, and computational efficiency, overcoming many of the limitations associated with classical methods.

2 Modeling Nonlinear Systems using FOHM

In this study, the nonlinear system is modeled using a Hammerstein structure, in which the static nonlinearity is represented by an exponential function. Specifically, the input signal $u(k)$ is first transformed by the function $f(u)$, enabling the model to capture strongly nonlinear behaviors commonly observed in many real processes. The resulting nonlinear signal, denoted $v(k)$, is then applied to a linear dynamic block, characterized by a fractional transfer function $H(s)$.

This process is illustrated in the functional diagram shown in Figure 1.

$$\boldsymbol{u(k)} \xrightarrow{f(u)=ae^{bu}+c} \boldsymbol{v(k)} \xrightarrow{H(z)} \boldsymbol{y(k)}$$

Fig. 1: Schematic structure of the model

This configuration combines the flexibility of the exponential nonlinearity with the richness of fractional-order dynamics, providing an effective representation of systems exhibiting both pronounced nonlinear behavior and complex dynamic properties.

The FOHM structure is defined by the following system of equations:

$$\begin{cases} f(u) = ae^{bu} + c \\ H(s) = \frac{y(s)}{v(s)} = \frac{b_M s^{M\alpha} + b_{M-1} s^{(M-1)\alpha} + \dots + b_0}{a_L s^{L\alpha} + a_{L-1} s^{(L-1)\alpha} + \dots + 1} \end{cases} \quad (1)$$

Where $a_1, \ldots, a_L, b_0, \ldots, b_M$ are constant coefficients and α is the commensurate fractional order with ($0 < \alpha < 1$). $a_1, \ldots, a_L, b_0, \ldots, b_M$, a, b, c and α are the parameters to be identified. These parameters are assembled in the vector X as follows:

$X = [a, b, c, a_1, \ldots, a_L, b_0, \ldots, b_M, \alpha]$

The transfer function $H(s)$ will be discretized using the Grunwald–Letnikov approximation[26] [28]. Therefore, it must be converted into a differential equation representing the relationship between the intermediate signal $v(k)$, and the output $y(t)$, as expressed in equation (2).

$$y(t) + \sum_{l=1}^{L} a_l D_t^{l\alpha} y(t) = \sum_{m=1}^{M} b_m D_t^{m\alpha} v(t) \quad (2)$$

where $D_t^{l\alpha}$ denotes the fractional-derivative operator, and L and M represent the number of fractional derivatives applied, respectively, to the output $y(t)$ and the intermediate signal $v(k)$.

$$D_t^{l\alpha} y(t) = \frac{1}{h^{l\alpha}} \sum_{i=0}^{(\frac{t}{h})} (-1)^i \binom{l\alpha}{i} y(t - ih) \quad (3)$$

$$D_t^{m\alpha} v(t) = \frac{1}{h^{m\alpha}} \sum_{i=0}^{(\frac{t}{h})} (-1)^i \binom{m\alpha}{i} v(t - ih) \quad (4)$$

where $\binom{l\alpha}{i}$ and $\binom{m\alpha}{i}$ are Newton's binomials generalized to noninteger orders, expressed by the following expressions.

$$\binom{l\alpha}{i} = \frac{l\alpha(l\alpha-1)\ldots(l\alpha-i+1)}{i!} \quad (5)$$

$$\binom{m\alpha}{i} = \frac{m\alpha(m\alpha-1)\ldots(m\alpha-i+1)}{i!} \quad (6)$$

The resulting expression is then sampled at time instants $t_k = kh$, where $k \in N^+$ and $h \in R^+$ denotes the sampling period. This yields the following expressions:

$$D_t^{l\alpha} y(k) = \frac{1}{h^{l\alpha}} \sum_{i=0}^{N_k} (-1)^i \binom{l\alpha}{i} y(k-i) \quad (7)$$

$$D_t^{m\alpha} v(k) = \frac{1}{h^{m\alpha}} \sum_{i=0}^{N_k} (-1)^i \binom{m\alpha}{i} v(k-i) \quad (8)$$

N_k denotes the number of past measurements taken into account in the computation of $y(k)$ and $v(k)$. By substituting expressions (7) and (8) into equation (2), the recursive equation is obtained, which is used to model and simulate the linear part of the FOHM.

Modeling processes with a Hammerstein structure involves identifying the model parameters, assembled in the vector X, using a set of N_h input–output measurements collected from the system.

The parameter estimation is performed by minimizing the quadratic criterion J_h. This criterion represents the sum of squared differences between the real system behavior $y_m(k)$ and the response $y(k)$ produced by the estimated model. The mathematical formulation of this optimization criterion is provided in equation (9).

$$J_h(X) = \sum_{i=1}^{N_h} (y(i) - y_m(i))^2 \quad (9)$$

3 Identification of the FOHM using HBA

The parameters of the FOHM model are obtained by searching for the vector X that minimizes the cost function J_h using the HBA[29][30], an optimization method inspired by the foraging behavior of the honey badger. The algorithm alternates between an exploitation phase (digging), where it performs local search around the best solutions, and an exploration phase (honey), guided by attraction toward promising candidates. It relies on a population of agents whose positions are updated through stochastic rules, allowing the solution quality to improve progressively. The corresponding pseudocode is presented below.

Inputs:
- $f(x)$: objective function to minimize
- N : number of honey badgers (population size)
- $MaxIter$: maximum number of iterations
- $[l_b, u_b]$: lower and upper bounds of the search space

Initialization:
while $i \le N$ do
- Generate random solution $X_i \in [l_b, u_b]$
- Evaluate fitness $J_h(X_i) = f(X_i)$

end while
Identify the best solution X_{best}
Main Loop:
for iter = 1 to $MaxIter$ do
- Update density factor ρ:
  $\rho = \rho_0 \exp(-(\text{iter} / \text{MaxIter}))$
- Compute foraging force F:
  $F = 2 \text{ rand}() \rho$
- for each badger $i = 1$ to N do
- Generate random number $r \in [0, 1]$

if r < 0.5 then
Digging phase:
$X_{new} = X_{best} + \text{F rand}()(X_i - X_{best}) \cos(2\pi\text{rand}())$
else
Honey phase:
$X_{new} = X_i + F\, rand()\, (X_{best} - X_i) + randn()$
end if
- Apply bounds to X_{new}
- If $J_h(X_{new}) < J_h(X_i)$ then
  $X_i = X_{new}$
  If $J_h(X_{new}) < J_h(X_{best})$ then
  $X_{best} = X_{new}$

The solutions obtained by the HBA are subsequently refined using a deterministic approach, based on gradient-based optimization techniques that follow a descent direction computed from the gradient or its approximation.

The procedure for determining the MHOF parameters is outlined in the following algorithm.

Inputs: Measurements of the input and output ;
Initialization:
- Lower and upper bounds for the parameters
- Number of parameters to identify
- Maximum number of iterations
- Population size

Steps:
- Compute the cost function
- Search for the parameters using the HBA
- Refine the solution using a local search method

4 Experimental Results and Discussion

4.1 Description of the Experimental Platform

The electro-thermal system shown in Figure 2 consists of an electric oven equipped with two heating resistors and two temperature sensors protected by a thermal insulation cylinder. Each heating resistor is powered by an alternating voltage, whose average value depends on the control voltage. The conversion between the DC control voltage and the AC voltage is performed by the single-phase dimmer SG444120, which supports a maximum current of 10A, has an input voltage range of 0–10V, and provides an output voltage ranging from 115 V to 265VAC.

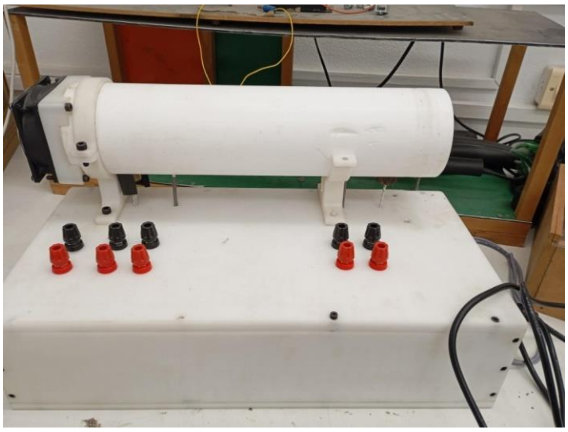

Fig. 2: The heating process.
Source: created by the authors

The input signals are applied to the thermal system and configured through the uVision editor and debugger, then implemented using the STM32 microcontroller from the STM32F407VG family. This microcontroller is based on the high-performance 32-bit ARM Cortex-M4 RISC core, operating at frequencies up to 168 MHz.

4.2 Analysis of nonlinearity

The temperature inside the electric oven, shown in Figure 2, exhibits a nonlinear behavior. This observation is experimentally confirmed by applying different input voltage levels to the oven and analyzing the resulting temperature evolution $y(°C)$. The corresponding curves are presented in Figure 3.

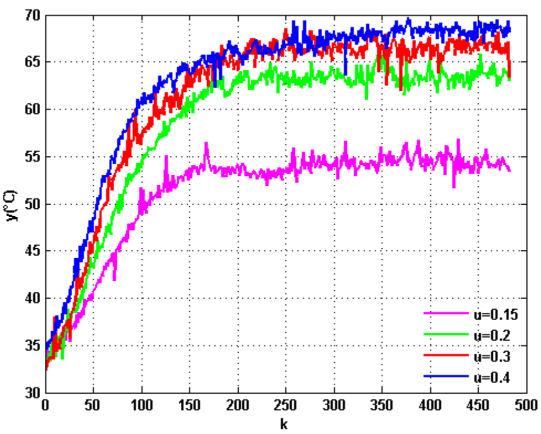

Fig. 3: Temperature response to varying supply voltages.
Source: created by the authors

The temperature variations shown in Figure 3 indicates that the system does not satisfy the superposition theorem, which states that for a system to be linear, the total response resulting from multiple inputs must be equal to the sum of the individual responses produced by each input applied separately.

4.3 Heating process modelling

The thermal system is modeled by FOHM based on experimental measurements of the system output, denoted y_m, which represents the temperature measured inside the electric oven, and the input, denoted u, corresponding to the DC voltage supplied by the digital-to-analog converter of the STM32F407VG microcontroller.

The thermal system was excited with step inputs $u(V)$ of different amplitudes (0.5 V; 0.1 V; 0.7 V; 0.2 V; 0.6 V; 0 V; 0.1 V; and 0.8 V), previously used in [13]. The measured temperature y_m (in degrees Celsius, °C) was recorded over a period of 5 hours and 18 minutes, with samples taken every 30 seconds (636 iterations). The experimental results obtained at each iteration k are plotted in Figure 4.

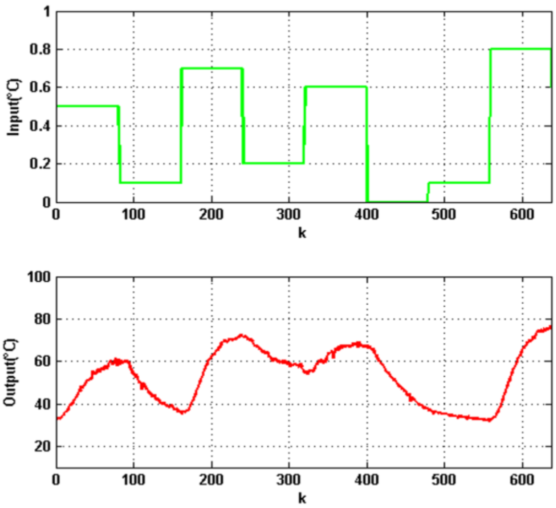

Fig. 4: The measured temperature y_m and the input sequence.
Source: created by the authors

The thermal system modeling using the MHOF approach consists in identifying the parameters of the static nonlinear block, which is modeled by a proposed exponential function, as well as the coefficients of the numerator and denominator of the fractional-order transfer function $H(s)$ representing the dynamic block, in addition to the fractional derivative order α.

This identification is carried out using experimental data related to the input u and the output y. These data correspond, respectively, to the voltage supplied by the digital-to-analog converter of the STM32F407VG microcontroller and to the temperature measured inside the electric oven.

In order to identify the most relevant structure for reproducing the dynamics of the thermal system, four models were considered.

Model 1:

$$\begin{cases} f_2(u) = ae^{bu} + c \\ H_2(s) = \dfrac{y(s)}{v(s)} = \dfrac{b_0}{a_1 s^\alpha + 1} \end{cases}$$

Model 2:

$$\begin{cases} f_2(u) = ae^{bu} + c \\ H_2(s) = \dfrac{y(s)}{v(s)} = \dfrac{b_1 s^\alpha + b_0}{a_2 s^{2\alpha} + a_1 s^\alpha + 1} \end{cases}$$

Model 3:

$$\begin{cases} f_3(u) = ae^{bu} + c \\ H_3(s) = \dfrac{y(s)}{v(s)} = \dfrac{b_2 s^{2\alpha} + b_1 s^\alpha + b_0}{a_3 s^{3\alpha} + a_2 s^{2\alpha} + a_1 s^\alpha + 1} \end{cases}$$

Model 4:

$$\begin{cases} f_4(u) = ae^{bu} + c \\ H_4(s) = \dfrac{y(s)}{v(s)} = \dfrac{b_3 s^{3\alpha} + b_2 s^{2\alpha} + b_1 s^\alpha + b_0}{a_4 s^{4\alpha} + a_3 s^{3\alpha} + a_2 s^{2\alpha} + a_1 s^\alpha + 1} \end{cases}$$

The parameters of HBA were set to ensure convergence, solution quality, and a reasonable computational time. The population size, representing the number of candidate solutions, was fixed at $N = 10$ in order to achieve a trade-off between exploration capability and computational cost. In addition, the maximum number of iterations was limited to $MaxIter = 50$ to reduce the overall computation time.

The respective lower bounds of the parameters a, b, c, b_3, b_2, b_1, b_0, a_4, a_3, a_2, a_1 and α are defined respectively as: 0.1, -0.5, -100, -1000, -1000, -1000, -1000, 0.1, 0.1 ,-1000, -1000, 0.5. Similarly, the corresponding upper bounds are given by: 10, 0.5, 100, 1000, 1000, 1000, 1000, 1000, 1000 , 1000, 1000, 1.5.

The parameters obtained using the HBA are subsequently refined through a fixed-step gradient descent approach to achieve faster convergence toward the optimal solution.

The parameters are estimated by applying the stochastic HBA using the measured output y_m and the input sequence u.
The estimated parameters are reported in Table 1.

Table 1. Identified Model Parameters and Associated Estimation Errors.

Models	Identified Parameters	Estimation Errors
Model 1	a=4.7968, b=-0.0482, c=-4.7585, b_0=-8.7027, a_1=80.3197, α =1.0232	0.0027
Model 2	a=4.5111, b=-0.0418, c=-4.4807, b_1=43.1944, b_0=-10.9964, a_2=5.6085, a_1=43.2597, α =0.8822	0.1219
Model 3	a=4.1301, b=0.0189, c=-4.1427, b_2=9.4340, b_1=-58.6914, b_0=24.6984, a_3=36.4428, a_2=33.5687, a_1=67.1350, α =0.9890	0.0025
Model 4	a=4.6136, b=-0.2335, c=-4.4354, b_3=-9.6134, b_2=-4.4048, b_1=7.3556, b_0=-2.3387, a_4=429.0005, a_3=428.9814, a_2=34.3923,a_1=31.6066, α=0.7765	0.0031

Source: created by the authors

Figure 5 illustrates the evolution curves of the measured temperature and the estimated temperature for each of the four proposed models.

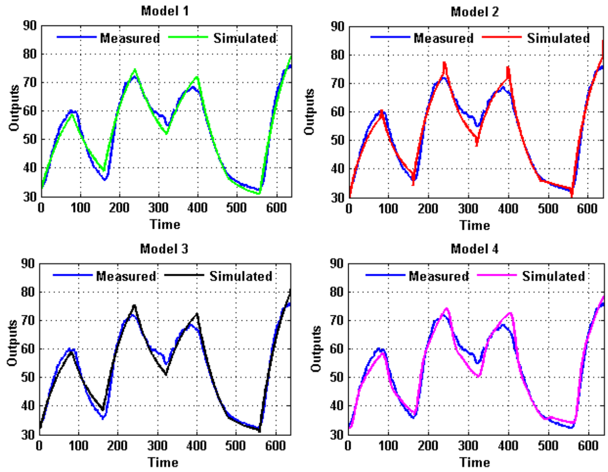

Fig. 5: The measured and the estimated temperature using HBA.
Source: created by the authors

According to Figure 5, it is clearly observed that the MHOF model incorporating an exponential static nonlinearity provides a temperature estimate that is in very good agreement with the experimental measurements. This model reproduces the dynamic behavior of the thermal system with satisfactory accuracy, which confirms its relevance for modeling the considered process. Furthermore, the results demonstrate the effectiveness of the stochastic HBA in solving a multivariable optimization problem and achieving reliable convergence toward the optimal solution.

In the following, the evolution of the parameters during the search for the optimal solution is simulated, and the corresponding curves are presented in Figure 6.

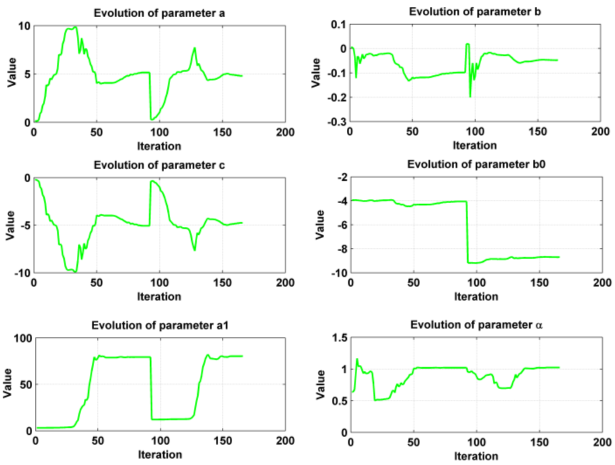

Fig. 6: The evolution of the parameters during the search for the optimal solution using HBA
Source: created by the authors

The analysis of the parameter evolution, illustrated in Figure 6, obtained using the HBA shows that the oscillations observed during the initial iterations are normal and reflect the global exploration phase of the search space. The gradual reduction of these oscillations, starting from iteration 135, indicates a transition toward a local exploitation phase around the optimal solution. Moreover, the parameters progressively converge to stable values, which confirms the ability of the HBA to reach an optimal solution. Finally, the fast convergence observed highlights the strong capability of the HBA to perform an efficient global search.

In order to illustrate the efficiency of the HBA, the model parameters were re-estimated using the geometric Nelder–Mead (NM) method[31][27] based on the simplex strategy. This procedure was carried out starting from exactly the same initial conditions as those adopted for the HBA, while maintaining the same constraints on the parameters. The evolution curves of the measured temperature and the estimated temperature for each of the four proposed models are illustrated by Figure 7.

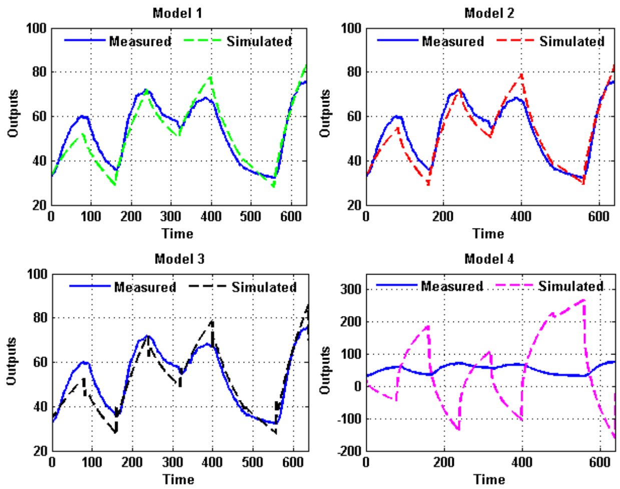

Fig. 7: The measured and the estimated temperature using NM approach.
Source: created by the authors

Figure 7 shows that the NM method provides a satisfactory estimation for Model 1, which is characterized by a relatively small number of parameters (6 parameters). However, its performance deteriorates for Model 4, where the parametric dimension is higher (12 parameters). It can therefore be concluded that the identification efficiency of the NM method decreases as the dimension of the search space increases. In contrast, HBA yields satisfactory estimations for all four studied models, as illustrated in Figure 5, which confirms its robustness with respect to an increasing number of parameters. This observation is further supported by the Root Mean Squared Error (RMSE) of the estimation errors, as given by the following expression:

$$\text{RMSE} = \sqrt{\frac{1}{N_h}\sum_{k=0}^{N_h}\left(y_m(k) - y(k)\right)^2} \qquad (10)$$

The estimation errors are computed for the four models using both optimization methods, which are summarized in Table 2.

Table 2. Estimation Errors for HBA and NM Identification Approaches.

Models	RMSE for HBA	RMSE for NM
Model 1	0.0519	0.1187
Model 2	0.3491	2.700
Model 3	0.05	3.2145
Model 4	0.0556	73.5014

Source: created by the authors

Table 2 shows that the HBA provides more accurate parameter estimations, particularly when the dimension of the search space is high. Indeed, HBA is a population-based metaheuristic method with strong global search capabilities, enabling it to efficiently explore the search space and avoid entrapment in local minima, especially for high-dimensional nonlinear problems. In contrast, the NM method is a deterministic local optimization technique based on a simplex strategy, which offers fast convergence when the initialization is close to the optimum but remains highly sensitive to initial conditions. Although NM generally exhibits lower computational complexity and rapid convergence for relatively smooth problems, its performance may deteriorate in the presence of strong nonlinearities or multiple local optima.

In the following, we focus on the computation time of the search procedure for both algorithms, NM and HBA. The corresponding results are summarized in Table 3.

Table 3. Computation time for HBA and NM Identification Approaches.

Models	**Computations time for HBA**	**Computations time for NM**
Model 1	28.8188	63.6270
Model 2	35.5711	131.7157
Model 3	68.5373	161.2092
Model 4	97.8126	43.8349

Source: created by the authors

The comparison of the two optimization approaches shows, first, that the computation time increases with the number of parameters to be estimated. An exception is observed for Model 4, for which the computation time decreases due to the divergence of NM algorithm. Second, the results indicate that the computation time of the HBA is significantly lower than that of NM method, highlighting the superior computational efficiency of the HBA and its ability to handle a large number of parameters within a reduced computation time.

5 Conclusion

In this work, we modeled a thermal system using a fractional-order Hammerstein structure, where the linear part is of exponential type. Unlike classical models, which represent the linear dynamics using polynomials, this approach leverages both fractional-order modeling and an exponential nonlinear function, avoiding the generation of multiple solutions when the estimated model is used in a control algorithm, such as predictive control.
Moreover, we employed the recent stochastic Honey Badger method for parameter estimation and demonstrated that it converges rapidly to the optimal solution due to its strong global search capability. We compared it with a classical optimization method, such as Nelder–Mead, and showed that the latter's performance deteriorates as the search dimension increases.

This work could be further improved by developing a control algorithm for real systems based on fractional-order Hammerstein structures with exponential nonlinearity.

Acknowledgement:
With deep gratitude, the author would like to thank the supervisor for his guidance and constant support during this research.

References:

[1] K. Geetha, P. Dinesh Kumar, Fractional-Order Mathematical Models for Heat Transfer in Advanced Thermal Systems, *Journal of Applied Mathematical Models in Engineering*, 1, 2, pp. 23–31, (2025).

[2] T. M. Elzaki, M. Z. Mohamed, A Novel Analytical Method for the Exact Solution of the Fractional-Order Biological Population Model, *Acta Mechanica et Automatica*, 18, 3, pp. 564 – 570, (2024), DOI: 10.2478/ama-2024-0059.

[3] E. Demir, I. Ozkol, Fractional-based nonlinear mechanical system modeling with FELEs: numerical analysis of oscillatory and nonoscillatory behavior of the inverted pendulum system, *Arch Appl Mech*, 95, 152, (2025), DOI: 10.1007/s00419-025-02860-1.

[4] W. Yanan , W. Min, D. Feng, Z. Daijiang, L. Chen, H. Xuebing, C. Yangquan, J. Changwei, Physics-Informed Fractional-Order Recurrent Neural Network for Fast Battery Degradation with Vehicle Charging Snippets, *Fractal Fract*, 9, 2, (2025), DOI: 10.1007/s00419-025-02860-1.

[5] K . Fan, Y. Jianfeng, X. Yijian, F. Junhua, A Volterra-series-based semi-analytical method for fractionally damped nonlinear systems under stochastic excitation, *Mechanical Systems and Signal Processing*, 241, 113579, (2025), DOI: 10.1016/j.ymssp.2025.113579.

[6] S M Sivalingam, V. Govindaraj, Neural fractional order differential equations, *Expert Systems with Applications*, 267, (2025), DOI: 10.1016/j.eswa.2024.126041.

[7] S.Fazzino, R. Caponetto, L. Patanè, A new model of Hopfield network with fractional-order neurons for parameter estimation.

Nonlinear Dyn 104, 2671–2685 (2021), DOI: 10.1007/s11071-021-06364-3.

[8] M. Ammara, R. Muhammad Asif Zahoor, N. Brett, Design of fractional-order hammerstein control auto-regressive model for heat exchanger system identification: Treatise on fuzzy evolutionary computing, *Chaos, Solitons & Fractals*, 181, (2025), DOI: 10.1016/j.chaos.2024.114644.

[9] L. Chunlei, W. Hongwei, Z. Qian, Simultaneous identification of parameters of fractional-order Hammerstein-Wiener model with time-delay using operational matrix in a colored noise environment, *Journal of the Franklin Institute*, 362, 1, (2025), DOI: 10.1016/j.jfranklin.2024.107444.

[10] C. Zhang, X. Meng, Y. Ji. Parameter Estimation of Fractional Wiener Systems with the Application of Photovoltaic Cell Model, *Mathematics*, 11, 13, (2023), DOI: 10.3390/math11132945.

[11] X. Yin, Y. Liu, A New Orthogonal Least Squares Identification Method for a Class of Fractional Hammerstein Models, *Algorithms*, 18, 4, (2025) , DOI: 10.3390/a18040201.

[12] V. Prasad, K. Kothari, U. Mehta, Parametric identification of nonlinear fractional Hammerstein models, *Fractal and Fractional*, 4, 1, pp. 1-12, (2020), DOI: 10.3390/fractalfract4010002.

[13] D. Chouaibi, W. Chagra, Nonlinear Predictive Control of Electric Oven Modelled by the *Fractional Hammerstein Structure, Part I: Journal of Systems and Control Engineering*, (2025), DOI: 10.1177/09596518251383234.

[14] K. Hammar, T. Djamah, M. Bettayeb, Fractional Hammerstein system identification based on two decomposition principles. *IFAC-PapersOnLine*, 52, 13, pp. 206-210, (2019), DOI: 10.1016/j.ifacol.2019.11.289.

[15] P. Vineet, M. Utkal, Modeling and parametric identification of Hammerstein systems with time delay and asymmetric dead-zones using fractional differential equations, *Mechanical Systems and Signal Processing*, 167, Part B, (2022), DOI: 10.1016/j.ymssp.2021.108568.

[16] J. A. Santos, G. L. O. Serra, Fuzzy Hammerstein Model Based State Space Identification Approach of Nonlinear Dynamic Systems, *WSEAS Transactions on Systems*, 17, pp. 89‑97, (2018).

[17] J. Rui, J. Li, Y. Chu, G. Lu, Parameter identification of fractional order Hammerstein model with two-stage piecewise nonlinearity based on iterative algorithms, *Measurement*, 203, 111951, (2022), DOI: 10.1016/j.measurement.2022.111951.

[18] M. Abd El‑Wanis, R. El‑Sehiemy, M. A. Hamida, Parameter Estimation of Permanent Magnet Synchronous Machines Using Particle Swarm Optimization Algorithm, Revue Roumaine des Sciences Techniques, *Série Électrotechnique et Énergétique*, 67, 4, pp. 377–382, (2022).

[19] R. Belal, M. Flitti, M. L. Zegai, Tuning of PI Speed Controller in Direct Torque Control of Dual Star Induction Motor Based on Genetic Algorithms and Neuro-Fuzzy Schemes, *Revue Roumaine des Sciences Techniques, Série Électrotechnique et Énergétique* , 69, 1, pp. 9–14, (2024).

[20] K. Kothari, U. Mehta, V. Prasad, J ; Vanualailai, Identification Scheme for Fractional Hammerstein Models With the Delayed Haar Wavelet, IEEE/CAA J. *Autom. Sinica*, 7, 3, pp. 882-891, (2020), DOI: 10.1109/JAS.2019.1911578.

[21] M. A. Ahmad, Z. Musa, M. H. Suid, M. Z. M. Tumari, Grey wolf optimizer for identification of liquid slosh behavior using continuous-time Hammerstein model, *Bulletin of Electrical Engineering and Informatics*, 9, 2, pp. 542–549, (2020), DOI: 10.11591/eei.v9i2.1720.

[22] Kubalčík, M., Bobál, V. Continuous-time and discrete multivariable decoupling controllers. *WSEAS Transactions on Systems and Control*, 9, (2014).

[23] B. Zhang, Z. Mao, Bias compensation principle based recursive least squares identification method for Hammerstein nonlinear systems, *Journal of the Franklin Institute*, 354, 3, pp. 1340-1355, (2017), DOI: 10.1016/j.jfranklin.2016.10.020.

[24] Z. Qian, H. Wang, C. Liu, Y. An, Establishment and identification of MIMO fractional Hammerstein model with colored noise, *Chaos, Solitons and Fractals*, 180, (2024), DOI: 10.1016/j.chaos.2024.114441.

[25] V. Prasad, K. Kothari, U. Mehta, Parametric identification of nonlinear fractional Hammerstein model, *Fractal and Fractional*, 4, 1, (2020), DOI: 10.3390/fractalfract4010002.

[26] D. Chouaibi, W. Chagra, A new hybrid optimization method used in predictive control of a nonlinear fractional model based on fractional Hammerstein structure, *Revue Roumaine des Sciences Techniques Série Électrotechnique et Énergétique*, 69, 4, pp. 437-448, (2024).

[27] D. Chouaibi, W. Chagra, Convex Optimisation in Nonlinear Predictive Control Based on Fractional Hammerstein Model, *8th International Conference on Mathematics and Computers in Sciences and Industry (MCSI)*, Athens, Greece, pp. 127-132, (2023), DOI: 10.1109/MCSI59815.2023.00029.

[28] A. Rhouma, F. Bouani, B. Bouzouita, M. Ksouri, Model predictive control of fractional order systems, *Journal of Computational and Nonlinear Dynamics*, 9, (2014), DOI: 10.1115/1.4026997.

[29] F. Hashim, E. Houssein, H. Hussain, K. Mabrouk, S. Mai, W. Al-Atabany, Honey Badger Algorithm: New metaheuristic algorithm for solving optimization problems, *Mathematics and Computers in Simulation*, 192, pp. 84–110, (2022), DOI: 10.1016/j.matcom.2021.08.013.

[30] P.Majumdar, S. Mitra, D. Bhattacharya, Honey Badger Algorithm using LENS opposition based learning and local search algorithm, *Evolving Systems*, pp. 1–26, (10 March 2023), DOI: 10.1007/s12530-023-09503-6.

[31] R.Fadhil, Z.A.H. Hassan, A hybrid Honey-Hadger Intelligence Algorithm with Nelder-Nead method and its application for reliability optimization, *International Journal of Intelligent Systems and Applications in Engineering*, 11, 4, pp. 136–145, (2023).

Contribution of Individual Authors to the Creation of a Scientific Article (Ghostwriting Policy)

The authors equally contributed in the present research, at all stages from the formulation of the problem to the final findings and solution.

Sources of Funding for Research Presented in a Scientific Article or Scientific Article Itself

No funding was received for conducting this study.

Conflict of Interest

The authors have no conflicts of interest to declare that are relevant to the content of this article.